Current Optics and Photonics
Vol. 3, No. 2, April 2019, pp. 172-176

ISSN: 2508-7266(Print) / ISSN: 2508-7274(Online)
DOI: https://doi.org/10.3807/COPP.2019.3.2.172

Optical Properties of a Proton-implanted Nd:CNGG Planar Waveguide

Qian-Lin Zhu, Ming-Fu Lin, Jing-Yi Chen, Zhong-Yue Wang, and Chun-Xiao Liu*

College of Electronic and Optical Engineering, Nanjing University of Posts and Telecommunications, Nanjing 210023, China

(Received September 24, 2018 : revised January 31, 2019 : accepted February 1, 2019)

The work reports on the fabrication of an optical planar waveguide in the Nd:CNGG crystal by the 0.4-MeV hydrogen ion implantation with a fluence of 8.0×10^{16} ions/cm^2. The nuclear energy loss of the implanted hydrogen ions was derived by using SRIM 2013 code. The microscope image of the proton-implanted Nd:CNGG crystal cross section was captured by a metallographic microscope. The transmittance spectra were recorded before and after the ion implantation. The light intensity distribution of the planar waveguide at 632.8 nm was experimentally measured to validate its effect on one dimension confinement. The investigation shows that the proton-implanted Nd:CNGG waveguide is a candidate for an optoelectronic integrated device.

Keywords : Ion implantation, Nd:CNGG crystal, Waveguide
OCIS codes : (230.7370) Waveguides; (220.4000) Microstructure fabrication

I. INTRODUCTION

An optical planar waveguide is one of the most basic components for integrated optical devices. It is a bridge for the propagation of optical signals between different parts of the optical circuit. A waveguide usually consists of a high refractive index core and two low refractive index cladding layers (One of the cladding layers is often air.). Such a structure can confine the light propagation within micro-scale volumes through internal total reflection, where the optical intensities can reach a much higher level. According to the different functions, the application of optical waveguides generally includes optical passive devices (such as waveguide couplers and waveguide isolators) and optical active devices (such as waveguide lasers and waveguide amplifiers) [1-9].

There are many different types of techniques for fabricating waveguides in optical materials, which mainly include diffusion of metal ions [10], ion exchange [11], ion implantation [12] and deposition of epitaxy layers [13]. Among these methods, ion implantation is one of the most competitive ways for modifying surface properties of optoelectronic materials. It has been employed to form waveguide structures in a lot of transparent materials because it offers the accurate control of both penetration depth and doping element by use of a particular species, as well as the energy of the ions [14]. The mechanism of an ion-implanted optical waveguide can be briefly described as follows. When ions are accelerated to a certain energy, they would be injected into the substrate, resulting in damage and defects. It leads to a change of refractive index and forms a waveguide layer on the near surface of the substrate [15]. In addition, proton implantation is one of the most attractive ion irradiation methods because the penetration depth of the proton implantation is the largest under the same conditions of implanted energy and target matrix [16].

Nd:$Ca_3(NbGa)_{2-x}Ga_3O_{12}$ or Nd:CNGG (neodymium-doped calcium niobium gallium garnet) is one of most outstanding disordered crystals [17]. Owing to the random distribution of vacancies and crystal lattices ions, Nd:CNGG performs better in some respects than Nd^{3+}-doped glasses and ordered crystals [18]. Its pump absorption band is broader than that of Nd-doped ordered crystals including Nd:YAG and Nd:YVO_4. The thermal conductivity of the Nd:CNGG crystal is higher than that of Nd^{3+}-doped glasses (Nd^{3+}-doped

*Corresponding author: chunxiaoliu@njupt.edu.cn, ORCID 0000-0003-1826-7048
Color versions of one or more of the figures in this paper are available online.

silicate and phosphate glasses). Therefore, the Nd:CNGG crystal has attracted more and more attention in the last decades. For example, the quasi-three-level continuous wave laser operation was generated based on the ultrafast-laser inscribed Nd:CNGG waveguides [19] and the high-power dual-wavelength laser was demonstrated in the Nd:CNGG crystal [20]. Moreover, the Nd:CNGG crystal waveguide was manufactured by the 480-keV proton implantation with a fluence of 1.0×10^{17} ions/cm^2 [21]. However, the near-field light intensity distribution of the proton-implanted Nd:CNGG waveguide could not be obtained by the end-face coupling technique. Furthermore, the measured near-field intensity profile is a direct and effective way to judge whether the light can propagate inside the waveguide region. Therefore, it is necessary to investigate the reason why the Nd:CNGG waveguide formed by the 480-keV proton implantation with a dose of 1.0×10^{17} ions/cm^2 does not get the near-field light intensity distribution and to explore new implantation conditions to achieve confinement of the guided mode. After our investigation and argumentation, it may be because the implanted dose is too high (1.0×10^{17} ions/cm^2) in Ref. [21]. In this work, although the optical waveguide is formed on the Nd:CNGG crystal by the same proton implantation, the energy and dose of the implantation are adjusted to obtain the near-field intensity profile. The proton implantation conditions are an energy of 0.4 MeV and a fluence of 8.0×10^{16} ions/cm^2. The mode image of the Nd:CNGG waveguide was measured by means of the end-face coupling system.

II. EXPERIMENTS AND SIMULATIONS

The Nd:CNGG crystal was grown by the Czochralski method at Shandong University. The crystal was cut to the size of 10 mm × 5 mm × 2 mm with two end-facets (5 mm × 2 mm) and two surfaces (10 mm × 5 mm) polished for the fabrication and characteristics of the Nd:CNGG waveguide. After the preparation conditions of the waveguide were calculated by the SRIM 2013 code, the 0.4-MeV

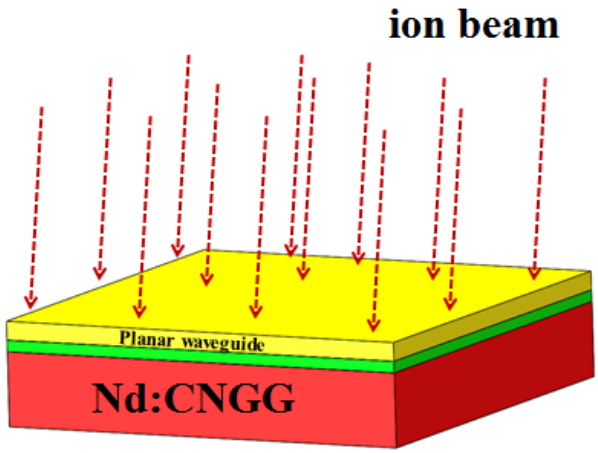

FIG. 1. Schematic of the proton implantation into the Nd:CNGG crystal.

protons with a fluence of 8.0×10^{16} ions/cm^2 were implanted into the Nd:CNGG crystal. Figure 1 shows the schematic of the proton implantation process. The ion implantation was performed on an implantor at Nanaln (Jinan Jingzheng Electronics Co., Ltd.).

The structure of the ion-implanted Nd:CNGG crystal was examined by a metallographic microscope. The absorption spectra of the Nd:CNGG crystal at room temperature in the wavelength range of 500-1000 nm were measured by means of a UV-VIS-NIR JASCO U-570 spectrophotometer before and after the hydrogen ion implantation.

Figure 2 shows the experimental setup for measuring the near-field intensity distribution. In the end-facet coupling experiment, an objective lens (or an optical fiber) was utilized to focus the light on the polished end-facet of an optical waveguide. The coupled light excited guided modes to propagate in the waveguide region. Then, another objective lens was employed to focus the output light from the other end-facet of the waveguide structure on an imaging device (a light screen or a CCD). The waveguide and the two lenses were all located on three-dimensional translation stages, as shown in the inset of Fig. 2.

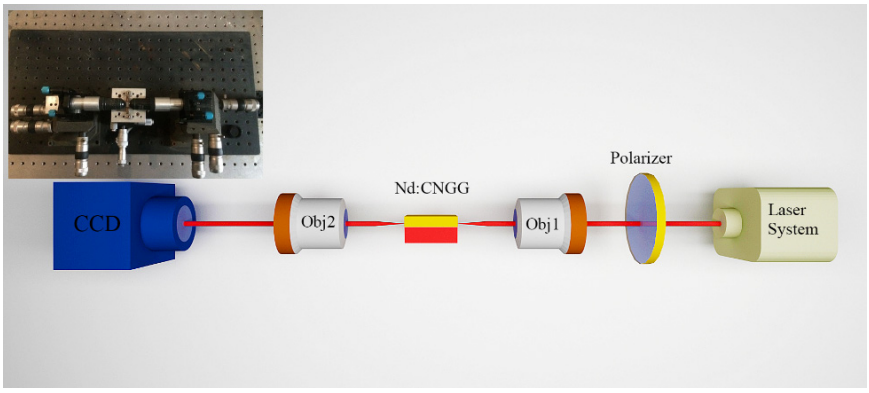

FIG. 2. Schematic diagram of the end-face coupling method. The inset is the photograph of the core components.

III. RESULTS AND DISCUSSION

The Nd:CNGG crystal after the hydrogen-ion implantation is shown in the inset of Fig. 3. The 10 mm × 2 mm facet pointed by the arrows was the surface on which the proton implantation was conducted. When the energetic hydrogen ions were implanted into the Nd:CNGG crystal, they would experience energy loss in the path towards the inner part of the crystal. The energy loss distribution was simulated through the SRIM 2013 code developed by James F. Ziegler [22, 23], as shown in Fig. 3. The maximum of nuclear energy loss is about 2.3 keV/μm at a depth of 2.87 μm. The decelerated ions would collide with the nucleus of the Nd:CNGG crystal and eventually stop. It makes the atoms of the crystal happen to shift, resulting in the crystal lattice damage. The density and refractive index in the damaged region are reduced to a certain extent, hence an optical barrier is formed.

Figure 4(a) is the photograph of a metallographic microscope that was used in the present work. The magnification of the microscope is ×500. Figure 4(b) shows the cross-sectional image of the planar Nd:CNGG waveguide taken by the metallographic microscope under reflected light. There is a certain color difference in the ion-implanted region, which is caused by a change in the refractive index. There is a negative refractive index change at the end of the ion-implanted profile. As shown in Fig. 4(b), the stripe is the waveguide core, whose refractive index is larger than that of air and the optical barrier. The thickness of the waveguide layer is approximately measured to be 2.8 μm. It is close to the simulated projection range of the 0.4-MeV protons in the Nd:CNGG crystal in Fig. 3. In addition, low-quality polishing results in discontinuities in the waveguide layer and some shallow pits on the surface of the Nd:CNGG crystal.

The guided mode pattern of the planar waveguide produced by virtue of the proton implantation with an energy of 0.4 MeV and a fluence of 8.0×10^{16} ions/cm^2 in the Nd:CNGG crystal was captured by the end-face coupling system at TE polarization, as shown in Fig. 5. Though there is a little light leaked into the substrate and air layers, a continuous and bright line on the photograph suggests that the light field could be confined in the waveguide region. The poor polishing results in the unevenness

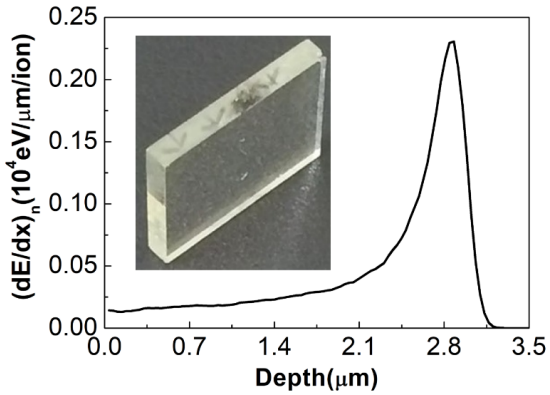

FIG. 3. Energy loss profile for the 0.4-MeV proton implantation into the Nd:CNGG crystal. The inset is the photograph of the implanted sample.

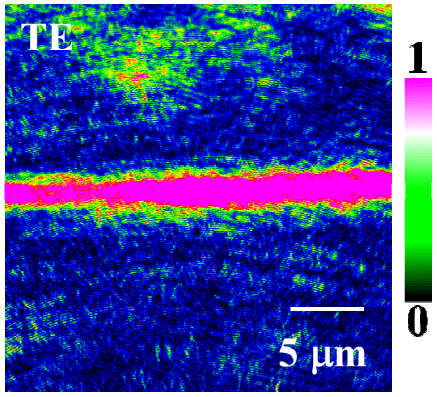

FIG. 5. Side view mode image of the waveguide detected by a CCD camera.

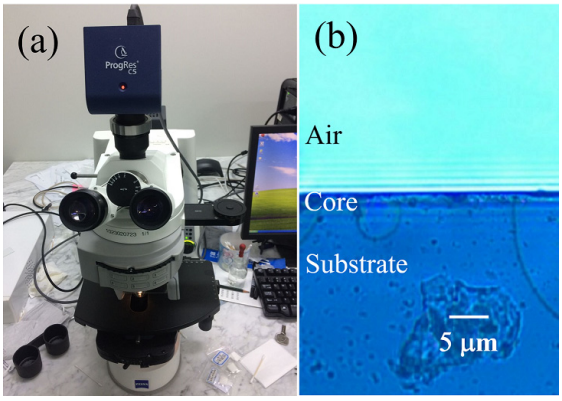

FIG. 4. (a) Photo of a metallographic microscope and (b) a cross-sectional view of the planar waveguide structure.

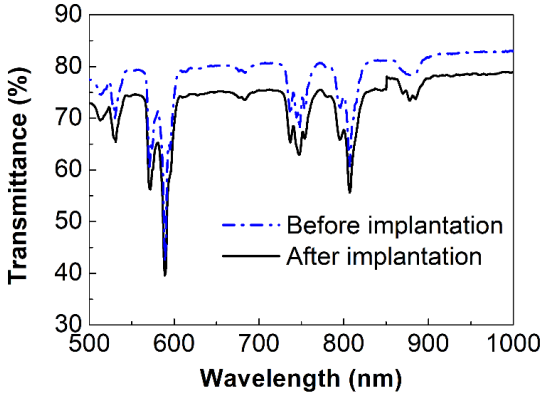

FIG. 6. Absorption spectra of the Nd:CNGG crystal before (dashed curve) and after (solid curve) the proton implantation.

of the bright line. Compared with the 1.0×10^{17}-ions/cm^2 proton-implanted Nd:CNGG waveguide, the waveguide manufactured by the hydrogen-ion implantation with a fluence of 8.0×10^{16} ions/cm^2 can confine the propagation of light. Therefore, the fabrication parameters are optimized in this work. Propagation loss plays a decisive role in the optical performances of a waveguide. The propagation loss of the proton-implanted Nd:CNGG waveguide was estimated to be 4.8 dB/cm by the back-reflection method [24, 25].

Figure 6 shows the absorption spectra of the unimplanted and as-implanted Nd:CNGG crystals. The thickness for the light transmission is 2.0 mm. As can be seen, the shape of the transmittance spectrum obtained from the implanted Nd:CNGG highly resembles that of the virgin crystal. The Nd:CNGG crystal before and after the ion implantation exhibits three main absorption bands centered at 588, 747 and 807 nm. They are due to the appropriate electronic transitions of Nd^{3+} ions: $^4I_{9/2} \rightarrow {}^2G_{7/2}+{}^4G_{5/2}+{}^2H_{11/2}$, $^4S_{3/2}+{}^4F_{7/2}$, and $^4F_{5/2}+{}^2H_{9/2}$. In addition, the transparent rate decreases slightly after the ion irradiation, which may be caused by the ion-implantation induced damage. It is consistent with the simulation of the SRIM 2013.

IV. CONCLUSION

In conclusion, a planar waveguide was formed in Nd:CNGG by the 0.4-MeV proton implantation with a dose of 8.0×10^{16} ions/cm^2. Its fabrication parameters were optimized, based on the previous report. A strip in the cross section of the hydrogen-ion implanted Nd:CNGG indicates a waveguide layer is constructed after the ion implantation. The near-field intensity profile suggests that the fundamental mode at 632.8 nm is supported by the proton-implanted Nd:CNGG waveguide. It is an improvement over the previously reported proton-implanted Nd:CNGG waveguide that cannot directly confine the light propagation.

ACKNOWLEDGMENT

The authors acknowledge the National Natural Science Foundation of China (Grant Nos. 11405041 and 51502144).

REFERENCES

1. I. Bányász, Z. Zolnai, M. Fried, S. Berneschi, S. Pelli, and G. Nunzi-Conti, "Leaky mode suppression in planar optical waveguides written in Er:TeO_2-WO_3 glass and CaF_2 crystal via double energy implantation with MeV N^+ ions," Nucl. Instrum. Methods Phys. Res., Sect. B **326**, 81-85 (2014).
2. G. S. Seo and T. J. Ahn, "Protection method for diameter downsized fiber Bragg gratings for highly sensitive ultraviolet light sensors," Curr. Opt. Photon. **2**, 221-225 (2018).
3. M. Zhang, C. Wang, R. Cheng, A. Shams-Ansari, and M. Loncar, "Monolithic ultra-high-Q lithium niobate microring resonator," Optica **4**, 1536-1537 (2017).
4. Y. Tan, X. B. Liu, Z. L. He, Y. R. Liu, M. W. Zhao, H. Zhang, and F. Chen, "Tuning of interlayer coupling in large-area graphene/WSe_2 van der Waals Heterostructure via ion irradiation: optical evidences and photonic applications," ACS Photonics **4**, 1531-1538 (2017).
5. J. D. B. Bradley and M. Pollnau, "Erbium-doped integrated waveguide amplifiers and lasers," Laser Photon. Rev. **5**, 368-403 (2011).
6. X. H. Li, X. M. Liu, D. Mao, X. H. Hu, and H. Lu, "Tunable and switchable multiwavelength fiber lasers with broadband range based on nonlinear polarization rotation technique," Opt. Eng. **49**, 094301-094304 (2010).
7. Y. Wang, X. L. Shen, R. L. Zheng, P. Lv, C. X. Liu, and H. T. Guo, "Optical planar waveguides fabricated by using carbon ion implantation in terbium gallium garnet," J. Korean Phys. Soc. **72**, 765-769 (2018).
8. Y. Tan, L. N. Ma, S. Akhmadaliev, S. Q. Zhou, and F. Chen, "Ion irradiated Er:YAG ceramic cladding waveguide amplifier in C and L bands," Opt. Mater. Express **6**, 711-716 (2016).
9. X. L. Shen, Q. F. Zhu, R. L. Zheng, P. Lv, H. T. Guo, and C. X. Liu, "Near-infrared optical properties of Yb^{3+}-doped silicate glass waveguides prepared by double-energy proton implantation," Results Phys. **8**, 352-356 (2018).
10. H. Hu, R. Ricken, and W. Sohler, "Low-loss ridge waveguides on lithium niobate fabricated by local diffusion doping with titanium," Appl. Phys. B **98**, 677-679 (2010).
11. A. Tervonen, B. R. West, and S. Honkanen, "Ion-exchanged glass waveguide technology: a review," Opt. Eng. **50**, 071107 (2011).
12. L. N. Ma, Y. Tan, M. Ghorbani-Asl, R. Boettger, S. Kretschmer, S. Zhou, Z. Huang, A. V. Krasheninnikov, and F. Chen, "Tailoring the optical properties of atomically-thin WS_2 via ion irradiation," Nanoscale **9**, 11027-11034 (2017).
13. F. Meriche, T. Touam, A. Chelouche, M. Dehimi, J. Solard, A. Fischer, A. Boudrioua, and L. H. Peng, "Post-annealing effects on the physical and optical waveguiding properties of RF sputtered ZnO thin films," Electron. Mater. Lett. **11**, 862-870 (2015).
14. F. Chen, "Micro- and submicrometric waveguiding structures in optical crystals produced by ion beams for photonic applications," Laser Photon. Rev. **6**, 622-640 (2012).
15. G. V. Vázquez, R. Valiente, S. Gómez-Salces, E. Flores-Romero, J. Rickards, and R. Trejo-Luna, "Carbon implanted waveguides in soda lime glass doped with Yb^{3+} and Er^{3+} for visible light emission," Opt. Laser Technol. **79**, 132-136 (2016).
16. D. Kip, "Photorefractive waveguides in oxide crystals: fabrication, properties, and applications," Appl. Phys. B **67**, 131-150 (1998).
17. C. X. Liu, L. L. Fu, L. L. Cheng, X. F. Zhu, S. B. Lin, R. L. Zheng, Z. G. Zhou, H. T. Guo, W. N. Li, and W. Wei, "Optimization effect of annealing treatment on oxygen-implanted Nd:CNGG waveguides," Mod. Phys. Lett. B **30**, 1650261 (2016).
18. P. K. Mukhopadhyay, K. Ranganathan, J. George, S. K. Sharma, and T. P. S. Nathan, "1.6 W of TEM_{00} cw output at 1.06 μm from Nd:CNGG laser end-pumped by a fiber-

coupled diode laser array," Opt. Laser Technol. **35**, 173-180 (2003).
19. Y. Tan, F. Chen, G. V. Vázquez, H. H. Yu, and H. J. Zhang, "Quasi-three-level laser emissions of neodymium-doped disordered crystal waveguides," IEEE J. Quantum Electron. **21**, 1601905 (2015).
20. H. H. Yu, H. J. Zhang, Z. P. Wang, J. Y. Wang, Y. G. Yu, Z. B. Shi, X. Y. Zhang, and M. H. Jiang, "High-power dual-wavelength laser with disordered Nd:CNGG crystals," Opt. Lett. **34**, 151-153 (2009).
21. C. X. Liu, M. Chen, L. L. Fu, R. L. Zheng, H. T. Guo, Z. G. Zhou, W. N. Li, S. B. Lin, and W. Wei, "Planar waveguides in neodymium-doped calcium niobium gallium garnet crystals produced by proton implantation," Chin. Phys. B **25**, 044211 (2016).
22. J. F. Ziegler, *SRIM - The stopping and range of ions in matter*, http://www.srim.org.
23. B. X. Xiang and L. Wang, "Near-infrared waveguide in gallium nitride single crystal produced by carbon ion implantation," Jpn. J. Appl. Phys. **56**, 050306 (2017).
24. R. Ramponi, R. Osellame, and M. Marangoni, "Two straightforward methods for the measurement of optical losses in planar waveguides," Rev. Sci. Instrum. **73**, 1117-1121 (2002).
25. L. Wang, C. E. Haunhorst, M. F. Volk, F. Chen, and D. Kip, "Quasi-phase-matched frequency conversion in ridge waveguides fabricated by ion implantation and diamond dicing of MgO:$LiNbO_3$ crystals," Opt. Express **23**, 30188-30194 (2015).